Open access • Journal Article • DOI:10.3390/EN11082107

Optimal P-Q Control of Grid-Connected Inverters in a Microgrid Based on Adaptive Population Extremal Optimization — Source link

Min-Rong Chen, Huan Wang, Guo-Qiang Zeng, Yuxing Dai ...+1 more authors

Published on: 13 Aug 2018 - Energies (Multidisciplinary Digital Publishing Institute)

Topics: Microgrid, AC power, Extremal optimization, Particle swarm optimization and Population

energies

MDPI

Article

Optimal P-Q Control of Grid-Connected Inverters in a Microgrid Based on Adaptive Population Extremal Optimization

Min-Rong Chen [1], Huan Wang [2,3], Guo-Qiang Zeng [2,*], Yu-Xing Dai [2,3] and Da-Qiang Bi [4]

[1] School of Computer, South China Normal University, Guangzhou 510631, China; mrongchen@126.com
[2] National-Local Joint Engineering Laboratory of Digitalize Electrical Design Technology, Wenzhou University, Wenzhou 325035, China; wh83@wzu.edu.cn (H.W.); daiyx@hnu.edu.cn (Y.-X.D.)
[3] College of Electrical and Information Engineering, Hunan University, Changsha 410082, China
[4] State Key Laboratory of Power Systems and Department of Electrical Engineering, Tsinghua University, Beijing 100084, China; bidaqiang@tsinghua.edu.cn
* Correspondence: zenggq@wzu.edu.cn or zeng.guoqiang5@gmail.com

Received: 24 July 2018; Accepted: 9 August 2018; Published: 13 August 2018

Abstract: The optimal P-Q control issue of the active and reactive power for a microgrid in the grid-connected mode has attracted increasing interests recently. In this paper, an optimal active and reactive power control is developed for a three-phase grid-connected inverter in a microgrid by using an adaptive population-based extremal optimization algorithm (APEO). Firstly, the optimal P-Q control issue of grid-connected inverters in a microgrid is formulated as a constrained optimization problem, where six parameters of three decoupled PI controllers are real-coded as the decision variables, and the integral time absolute error (ITAE) between the output and referenced active power and the ITAE between the output and referenced reactive power are weighted as the objective function. Then, an effective and efficient APEO algorithm with an adaptive mutation operation is proposed for solving this constrained optimization problem. The simulation and experiments for a 3 kW three-phase grid-connected inverter under both nominal and variable reference active power values have shown that the proposed APEO-based P-Q control method outperforms the traditional Z-N empirical method, the adaptive genetic algorithm-based, and particle swarm optimization-based P-Q control methods.

Keywords: power control; grid-connected inverter; extremal optimization; design optimization; evolutionary algorithms

1. Introduction

As an important distribution system, a microgrid integrates a variety of renewable and traditional distributed generations and different loads [1]. How to design optimal controllers to guarantee that the microgrid operates well in both islanded and grid-connected modes is one of the critical issues in the microgrid research area [2–6]. More specifically, it is important to control the voltage and frequency of each power converter connected to each distributed generation, called the VF control, in the islanded mode while it is necessary to regulate the output active and reactive powers of each distributed generation, called the P-Q control in the grid-connected mode. Some recent works have studied the optimal voltage control issue of the distribution systems in the presence of distributed energy resources [7,8]. This paper focuses on the optimal P-Q control issue of a microgrid in the grid-connected mode.

In the past decade, some P-Q control methods have been proposed for distributed generations [9–15]. Dai [9] developed an effective power flow control method for a distributed

generation unit in the grid-connected mode by adopting a robust servomechanism voltage controller and a discrete-time sliding mode current controller on the basis of Newton–Raphson-based parameter estimation and feed forward control approaches. The research work [11] studied the control problem of active and reactive powers using a second-order generalized integrator in a single-phase grid-connected fuel cell system based on the boost inverter. In Reference [12], an individual-phase decoupled P-Q control method based on six control degrees was proposed for a three-phase voltage source converter. Adhikari and Li [13] proposed a P-Q control method with solar photovoltaic, maximum power point tracking (MPPT), and battery storage in the grid-connected mode. Adhikari et al. [14] proposed a two-selected control method using theP-Q control in the load-following mode while the P-V control was in the maximum power point tracking mode. Unfortunately, the design processes of multivariable parameters used in P-Q controllers in the above works rely on deeply empirical rules of the engineers, so the performance under dynamic loads variations often becomes poorer. In fact, the design issue of P-Q controllers is essentially optimally solving a constrained optimization problem, but there are only a few reported works concerning the design of P-Q controllers from the perspectives of constrained optimization. Al-Saedi et al. [16] presented a particle swarm optimization (PSO)-based P-Q control method in grid-connected operation under variable loads conditions. This seminal work has demonstrated the importance of PSO in the automatic tuning of P-Q control parameters for optimized operation during abrupt loads change, but two current control parameters in the designed control system lack the optimization process based on PSO, so it may be considered as an incomplete optimization process for designing P-Q controllers. On the other hand, some popular evolutionary and swarm algorithms have been applied successfully to the optimal control of power converters and power systems [17–19], which motivate us to design an effective and efficient optimization algorithm to the optimal P-Q control issue of three-phase grid-connected inverters in a microgrid.

As a novel optimization framework originally inspired by the far-from-equilibrium dynamics of self-organized criticality (SOC) [20], extremal optimization (EO) [21,22] is different from other evolutionary algorithms because it merely selects against the bad instead of favoring the good based on a uniform random or power-law probability distribution. According to the iterated mechanism, EO can be classified into two categories. The first one is the individual-based discrete EO such as the standard EO [21,22] and the self-organized optimization algorithm [23,24] for combinatorial optimization problems, where an individual often represents a discrete sequence, e.g., a cyclic permutation of cities for the traveling salesman problem, and individual-based iterated operations including selection and discrete mutations, e.g., the 2-Opt, 3-Opt, and Lin–Kernighan (LK) rules for TSP are adopted. In the binary-coded EO (BCEO) algorithm [25], a set of decision variables of a continuous optimization problem are coded as a binary string, and the power law-based selection and binary mutation operate on this binary string. The second is the population-based continuous EO by using population iterated operations, e.g., polynomial mutations and multi-non-uniform mutations. A variety of simulation and experimental results on different kinds of benchmark and real-world engineering optimization problems have shown that EO and its modified algorithms perform better than or at least the same as other popular evolutionary algorithms such as genetic algorithm (GA) and PSO [26]. In the past decade, some modified EO algorithms have been applied to the optimal design issue of PID and fractional-order PID controllers for complex control systems [27–33]. To the best of the authors' knowledge, the applications of EO to the optimal P-Q control of power converters have never been reported.

Encouraged by the aforementioned analysis, a novel intelligent P-Q control method is proposed for three-phase grid-connected inverters in a microgrid by using an adaptive population-based extremal optimization (APEO). The proposed method formulates the optimal P-Q control issue of three-phase grid-connected inverters in a microgrid as a typical constrained optimization problem firstly, where six parameters of decoupled PI controllers are real-coded as the decision variables and the integral time absolute error (ITAE) between the output and referenced active power and the ITAE between the

output and referenced reactive power are weighted as the objective function. Then, an effective and efficient APEO algorithm with an adaptive mutation operation is proposed to solve this optimal issue.

The major contributions of this work are described as follows:

(1) To the best of the authors' knowledge, the adaptive population-based extremal optimization is applied firstly to the optimal P-Q control issue of three-phase grid-connected inverters in a microgrid.
(2) The superiority of the proposed method is demonstrated by both the simulation and experimental results for a three-phase grid-connected inverter in a microgrid. In fact, the previous reported PSO-based P-Q control method [16] was tested only using its simulation results.
(3) In cases of both nominal and variable reference active power values, the proposed APEO-based P-Q control method can improve the performance of a three-phase grid-connected inverter in a microgrid compared to the traditional Z-N empirical method, the adaptive GA-based, and the PSO-based P-Q control methods.

The rest of this paper is structured as follows. Section 2 presents the preliminaries concerning grid-connected inverters and extremal optimization. In Section 3, an intelligent P-Q control method is designed for grid-connected inverters in a microgrid based on adaptive population EO. Section 4 gives the simulation results on a three-phase grid-connected inverter. Moreover, in order to further validate the superiority of the proposed APEO-based P-Q control method, the experimental results on a real 3 kW three-phase grid-connected inverter in a microgrid are presented in Section 5. Finally, the conclusion and open problems are given in Section 6.

2. Problem Formulation

Figure 1 shows the circuit diagram and the corresponding P-Q control scheme for a three-phase grid-connected inverter in a microgrid [16,34]. Here, V_{dc} is the DC voltage provided by a distribution generation unit, C_d and C_f are the capacitance of the DC side and the LC filter, respectively, L_f represents the equivalent inductance of the LC filter, and R_f is the equivalent resistance of the LC filter. The P-Q control scheme consists of the following key operations: the grid-side voltage, a current and phase detector, an inverter-side voltage and current detector, active and reactive power calculation, an active power PI controller, a reactive power PI controller, a current PI controller, abc/dq and dq/abc transformations, and space vector pulse width modulation (SVPWM).

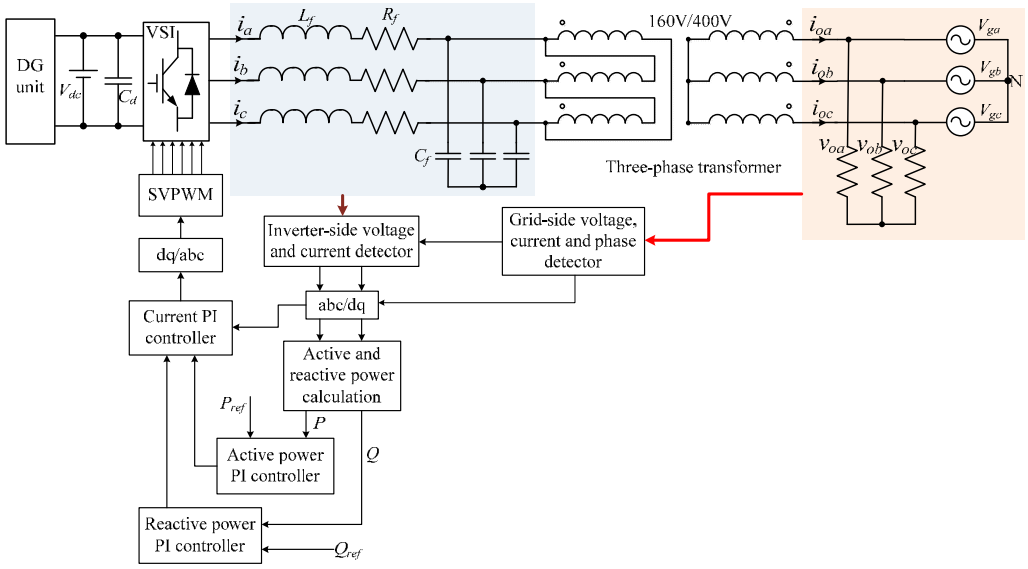

Figure 1. The P-Q control scheme of a three-phase grid-connected inverter in a microgrid.

The block diagram of decoupled P-Q controllers for a three-phase grid-connected inverter in a microgrid is presented in Figure 2. The active and reactive powers of the inverter denoted as P and Q, respectively, are computed as follows:

$$P = 1.5 \times (v_{od} \times i_{od} + v_{oq} \times i_{oq}) \tag{1}$$

$$Q = 1.5 \times (v_{oq} \times i_{od} - v_{od} \times i_{oq}) \tag{2}$$

where v_{od} and v_{oq} are the d-coordinate and q-coordinate of the grid-side voltage, respectively, and i_{od} and i_{oq} are the d-coordinate and q-coordinate of the grid-side current, respectively.

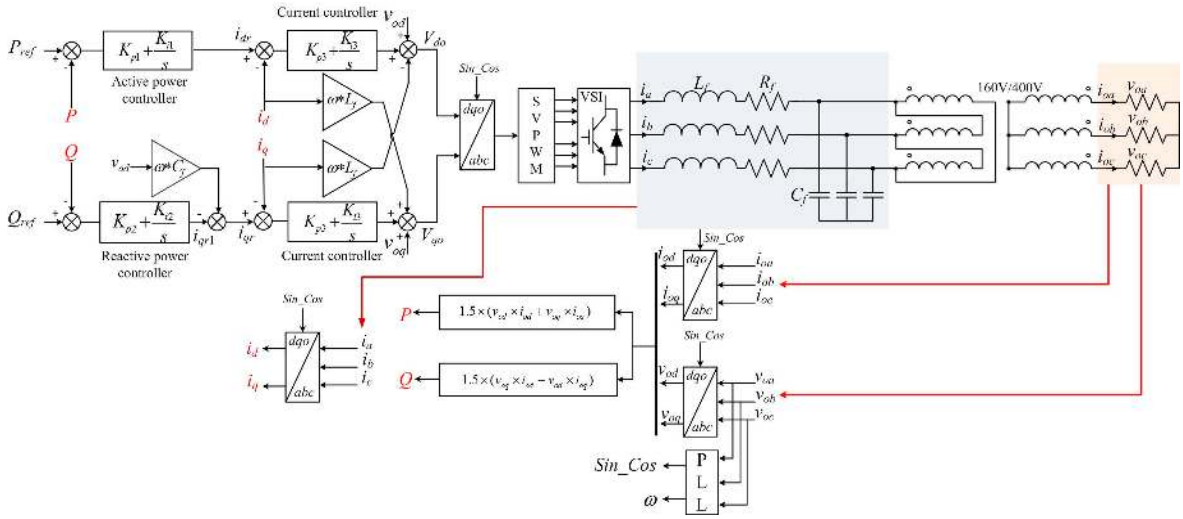

Figure 2. The block diagram of decoupled P-Q controllers for a three-phase grid-connected inverter in a microgrid.

The transfer functions of active and reactive power PI controllers denoted as $G_P(s)$ and $G_Q(s)$ are defined as follows:

$$G_P(s) = \frac{i_{dr}(s)}{P_{ref}(s) - P(s)} = K_{p1} + \frac{K_{i1}}{s} \tag{3}$$

$$Q = 1.5 \times (v_{oq} \times i_{od} - v_{od} \times i_{oq}) \tag{4}$$

where P_{ref} and Q_{ref} are the reference values of active and reactive powers, respectively; i_{dr} and i_{qr1} are the output values of the active and reactive PI controllers, respectively; K_{p1} and K_{i1} are the proportional and integral parameters of the active PI controller, respectively; K_{p2} and K_{i2} are the proportional and integral parameters of reactive PI controller, respectively.

The reference voltage signals in the dq frame of SVPWM is defined as follows:

$$\begin{bmatrix} V_{do} \\ V_{qo} \end{bmatrix} = \begin{bmatrix} -K_{p3} & -\omega L_f \\ \omega L_f & -K_{p3} \end{bmatrix} \begin{bmatrix} i_d \\ i_q \end{bmatrix} + \begin{bmatrix} K_{p3} & 0 \\ 0 & K_{p3} \end{bmatrix} \begin{bmatrix} i_{dr} \\ i_{qr} \end{bmatrix} + \begin{bmatrix} K_{i3} & 0 \\ 0 & K_{i3} \end{bmatrix} \begin{bmatrix} x_d \\ x_q \end{bmatrix} + \begin{bmatrix} v_{od} \\ v_{oq} \end{bmatrix} \tag{5}$$

$$x_d = (i_{dr} - i_d)/s \tag{6}$$

$$x_q = (i_{qr} - i_q)/s \tag{7}$$

where i_d and i_q are the d-coordinate and q-coordinate of the inverter-side current, respectively; K_{p3} and K_{i3} are the proportional and integral parameters of the current PI controller, respectively; w is the angular frequency; and i_{qr} is the reference input of the q-coordinate of the current PI controller, i.e., $i_{qr} = w \times C_f \times v_{od} - i_{qr1}$. Note that i_{dr} is also the reference input of the d-coordinate of the current PI controller.

In order to manage the active and reactive power of each distributed generation in a microgrid under the grid-connected mode, the design issue of an optimal P-Q controller with six parameters, including K_{p1}, K_{i1}, K_{p2}, K_{i2}, K_{p3}, and K_{i3}, can be formulated as a typical constrained optimization problem. More specifically, six parameters of decoupled PI controllers are real-coded as decision variables and the integral time absolute error (ITAE) between the output and referenced active power and the ITAE between the output and referenced reactive power are weighted as a minimized function. The complete formulation of the optimal P-Q control issue for a three-phase grid-connected inverter is as follows:

$$\begin{gathered} \min F(\mathbf{x}) = w_1 \int_0^{T_{\max}} t\left|P_{ref} - P\right| dt + w_2 \int_0^{T_{\max}} t\left|Q_{ref} - Q\right| dt \\ \mathbf{x} = (K_{p1}, K_{i1}, K_{p2}, K_{i2}, K_{p3}, K_{i3}) \\ \text{s.t. Equations } (1) \sim (7) \\ l_1 \le K_{p1} \le u_1 \\ l_2 \le K_{i1} \le u_2 \\ l_3 \le K_{p2} \le u_3 \\ l_4 \le K_{i2} \le u_4 \\ l_5 \le K_{p3} \le u_5 \\ l_6 \le K_{i3} \le u_6 \end{gathered} \tag{8}$$

where P_{ref} and Q_{ref} are the referenced active and reactive powers, respectively; w_1 and w_2 are the weighted coefficients; $T_{\max}$ is the maximum time of the time window; l_1, l_2, l_3, l_4, l_5, and l_6 are the lower limits of K_{p1}, K_{i1}, K_{p2}, K_{i2}, K_{p3}, and K_{i3}, respectively; and u_1, u_2, u_3, u_4, u_5, and u_6 are the upper limits of K_{p1}, K_{i1}, K_{p2}, K_{i2}, K_{p3}, and K_{i3}, respectively.

3. The Proposed Method

In this section, an intelligent P-Q control method is presented for three-phase grid-connected inverters in a microgrid by using an adaptive population-based extremal optimization algorithm (APEO). The key idea behind the proposed method is firstly formulating the optimal P-Q control of grid-connected inverters in a microgrid as a typical constrained optimization problem shown as Equation (8). Then, an effective and efficient APEO algorithm with an adaptive mutation operation is designed to solve this optimization problem.

The detailed steps of the proposed algorithm are described as follows:

Input: The model of a three-phase grid-connected inverter with P-Q controllers, a sampling period T_s, the lower limits constraints (l_1, l_2, l_3, l_4, l_5, l_6) and upper limits constraints (u_1, u_2, u_3, u_4, u_5, u_6) of the P-Q control parameters (K_{p1}, K_{i1}, K_{p2}, K_{i2}, K_{p3}, K_{i3}), the weight coefficients w_1 and w_2 used for evaluating the objective function, a population size of N, the maximum number of iterations $I_{\max}$, and the shape parameter b of the adaptive mutation operation.

Output: The best solution S_{best} (the best control parameters K_{po1}, K_{io1}, K_{po2}, K_{io2}, K_{po3}, K_{io3}), the corresponding global fitness F_{best}, the real-time curve of the active and reactive power, and the current waveform of the transformer.

Step1: Generate a random initial real-coded population $\boldsymbol{P_I} = \{S_1, S_2, \ldots, S_N\}$, where the population size N is generally set as an even number, each solution S_i represents a real-coded sequence of six control parameters including K_{p1}, K_{i1}, K_{p2}, K_{i2}, K_{p3}, K_{i3}, and set $\boldsymbol{P} = \boldsymbol{P_I}$. More specifically, the generated process of S_i is $S_i = L + R_i(U - L),\ i = 1, 2, \ldots, N$, where $L = (l_1, l_2, l_3, l_4, l_5, l_6)$ and $U = (u_1, u_2, u_3, u_4, u_5, u_6)$, and R_i is a set of randomly generated values between 0 and 1.

Step 2: Evaluate the fitness $\{F_i, i = 1, 2, \ldots, N\}$ of each solution S_i in population $\boldsymbol{P}$ by means of Equation (8) firstly. Then rank all the solutions $\{S_i, i = 1, 2, \ldots, N\}$ in ascending order of the fitness values $\{F_i, i = 1, 2, \ldots, N\}$, which means obtaining a permutation Π of the labels i such that. Set the best fitness of the current iteration as $F_{\text{best}} = F_{\Pi(1)}$ and the corresponding best solution $S_{\text{best}} = S_{\Pi(1)}$.

Step3: Select the solutions whose fitness ranks are from $\Pi(1)$ to $\Pi(N/2)$ to replace those solution whose fitness rank from $\Pi(1+N/2)$ to $\Pi(N)$, and set the intermediate population $\boldsymbol{P_M} = \{S_{M1}, S_{M2}, \ldots, S_{MN}\}$, where $S_{Mj} = S_{M(j+N/2)} = S_{\Pi(j)}$, $j = 1, 2, \ldots, N/2$.

Step4: Generate a new population $\boldsymbol{P_N} = \{S_{N1}, S_{N2}, \ldots, S_{NN}\}$ from $\boldsymbol{P_M}$ by adopting a multi-non-uniform mutation (MNUM). To be more specific, S_{Ni} is computed by the following equations:

$$S_{Ni} = \begin{cases} S_{Mi} + (U - S_{Mi})A(t), & \text{if } r < 0.5 \text{ and } L \le S_{Ni} \le U; \\ S_{Mi} + (S_{Mi} - L)A(t), & \text{if } r \ge 0.5 \text{ and } L \le S_{Ni} \le U; \\ S_{Mi}, & \text{if } S_{Ni} < L \text{ or } S_{Ni} > U; \end{cases} \tag{9}$$

$$A(t) = \left[r_1 \left(1 - \frac{t}{I_{\max}} \right) \right]^b \tag{10}$$

where t is defined as the current number of iterations, r and r_1 are the randomly generated numbers between 0 and 1, and b represents the shape parameter, which adjusts the dynamics of the mutation operation.

Step 5: Set $S_{NN} = S_{\text{best}}$ and accept $\boldsymbol{P} = \boldsymbol{P_N}$ unconditionally.

Step 6: Repeat step 2 to step 5 until some stopping criterion, e.g., the maximum number of iterations $I_{\max}$, is satisfied.

Step 7: Output the best control parameters solution $S_{\text{best}} = (K_{po1}, K_{io1}, K_{po2}, K_{io2}, K_{po3}, K_{io3})$, the corresponding global fitness F_{best}, the real-time curve of the active and reactive power, and the current waveform of loads.

Figure 3 presents the flowchart of APEO-based P-Q controllers design algorithm for three-phase grid-connected inverters. From the design perspective of the evolutionary algorithm, the proposed APEO-based P-Q controller design algorithm for three-phase grid-connected inverters has only the selection and mutation operations. Moreover, the proposed APEO method has fewer adjustable parameters than the adaptive genetic algorithm (AGA) [35] and the particle swarm optimization (PSO) [16]. More specifically, except for the maximum number of iterations $I_{\max}$ and the population size N, only one shape parameter b needs to be tuned in the proposed APEO algorithm. However, two additional adjustable parameters in AGA and five additional parameters in PSO need be tuned for a specific practical three-phase grid-connected inverter. In this sense, the proposed APEO-based P-Q controller design algorithm can be considered as being simpler than the AGA and PSO-based P-Q control methods. In addition, the superiority of the proposed APEO method to the AGA and PSO-based P-Q algorithms will be verified by the simulation and experimental results on a three-phase grid-connected inverter in a microgrid under both nominal and variable reference active power values in the next two sections.

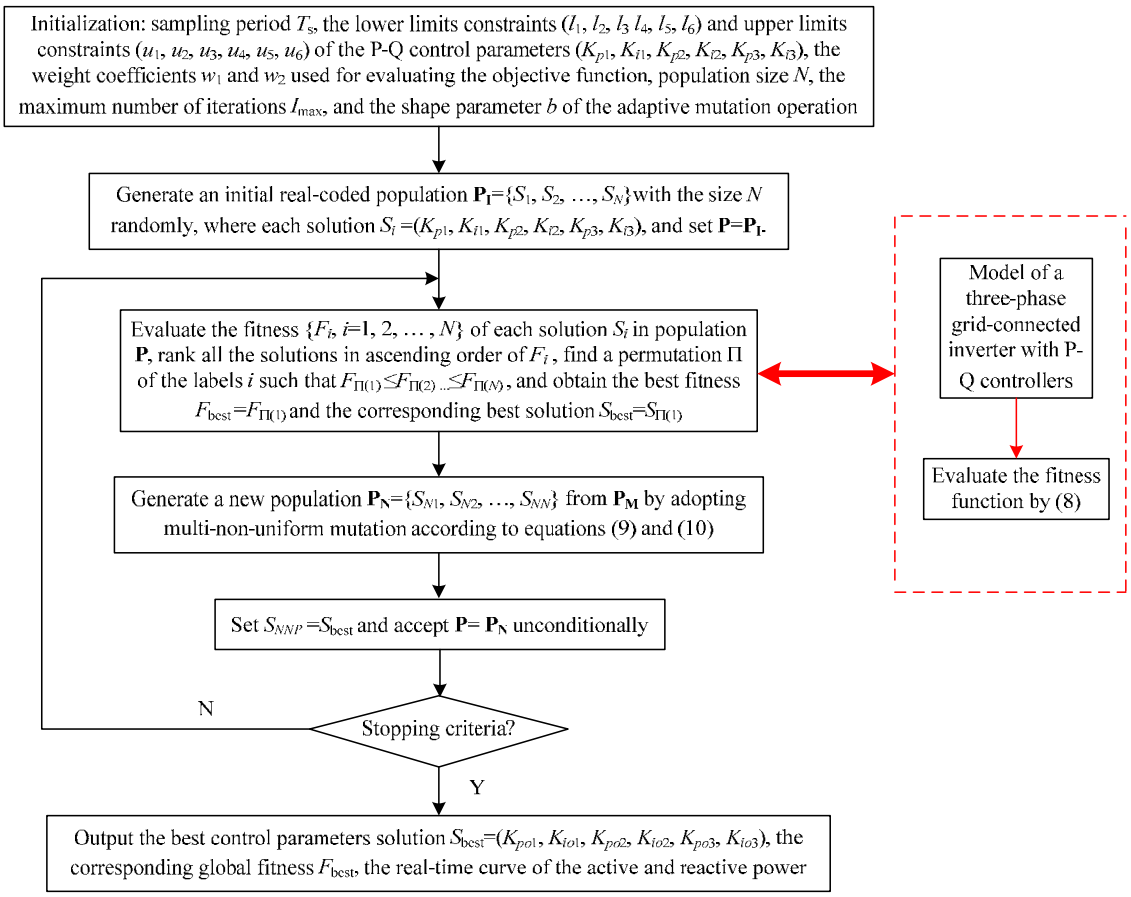

Figure 3. The flowchart of APEO-based P-Q controllers' design algorithm for three-phase grid-connected inverters.

4. Simulation Results

4.1. Test for Benchmark Functions

Here, five benchmark functions shown in Table 1 are chosen from the literature [36] to illustrate the superiority of the proposed APEO algorithm to other popular optimization algorithms, such as the genetic algorithm (GA) [36], PSO [36], the original population-based extremal optimization version with lévy mutation termed as PEO [37], the hybrid PSO-EO algorithm [36], and the real-coded PEO with polynomial mutation termed as RPEO-PLM [38]. For the fair comparison, the parameters settings of GA, PSO, PEO, PSO-EO, and RPEO-PLM algorithms are the same as those in Reference [36,38]. The shape parameter b used in the APEO algorithm is set as b = 5. The number of maximum iterations is set the same as that in References [36,38], which is 20,000 for F_1, F_2, and F_3; 10,000 for F_4;and 100,000 for F_5. Similarly, the popular size is set as follows: N = 10 for F_1 and F_3, and N = 30 for the other three functions. Each algorithm has been implemented by 20 independent runs for each function.

Table 2 compares the performance of APEO, GA, PSO, PEO, PSO-EO, and RPEO-PLM for the five test functions. Note that their performance is evaluated by the statistical results including the best values, average values, worst values, and the standard deviation of the 20 optimized fitness. The best performance is in bold. Clearly, APEO achieves the best performance for F_1, F_2, and F_5, and the same performance as PSO, PSO-EO, and RPEO-PLM yet better than GA and PSO for F_3 and F_4. As a consequence, APEO performs better than or at least competitive with GA, PSO, PEO, PSO-EO, and RPEO-PLM for the five test functions. In other words, APEO can be considered as more suitable than the other popular optimization algorithms for the optimal P-Q control issue of three-phase grid-connected inverters in a microgrid.

Table 1. The five benchmark functions.

Function	Function Expression	Search Space	n	Global Optimum
Michalewicz	$F_1 = -\sum_{i=1}^{n} \sin(x_i) \sin^{2m}(\frac{ix_i^2}{\pi}), m = 10$	$(0, \pi)^n$	10	−9.66 min
Schwefel	$F_2 = -\sum_{i=1}^{n} x_i \sin(\sqrt{x_i})$	$(-500, 500)^n$	30	−12,569.487 min
Rastrigin	$F_3 = \sum_{i=1}^{n} [x_i^2 - 10\cos(2\pi x_i) + 10]$	$(-5.12, 5.12)^n$	30	0 min
Ackley	$F_4 = 20 + e - 20\exp\left(-0.2\sqrt{\frac{1}{n}\sum_{i=1}^{n} x_i{}^2}\right) - \exp\left(\sum_{i=1}^{n} \frac{\cos(2\pi x_i)}{n}\right)$	$(-32.768, 32.768)^n$	30	0 min
Rosenbrock	$F_5 = \sum_{i=1}^{n-1} [100(x_{i+1} - x_i{}^2)^2 + (x_i - 1)^2]$	$(-30, 30)^n$	30	0 min

Table 2. The comparative performance of APEO and the other popular optimization algorithms for test functions.

Test Function	Algorithm	Best	Average	Worst	Standard Deviation	Rank
F_1	APEO	−9.66	−9.66	−9.66	1.45×10^{-15}	1
	RPEO-PLM [38]	−9.66	−9.66	−9.66	5.767×10^{-5}	2
	PSO-EO [36]	−9.66	−9.66	−9.66	2.15×10^{-3}	3
	PSO [36]	−9.66	−9.52	−9.06	0.17	6
	GA [36]	−9.66	−9.62	−9.50	0.06	4
	PEO [37]	−9.61	−9.55	−9.50	0.03	5
F_2	APEO	−12,569.5	−12,569.5	−12,569.5	1.82×10^{-5}	1
	RPEO-PLM [38]	−12,569.5	−12,569.5	−12,569.5	1.052×10^{-5}	2
	PSO-EO [36]	−12,569.5	−12,568.0	−12,562.6	2.01	3
	PSO [36]	−9577.7	−10,139.3	−11,026.2	625.7	5
	GA [36]	−9549.3	−8846.0	−8404.5	481.0	6
	PEO [37]	−12,214.2	−12,083.3	−11,977.3	90.3	4
F_3	APEO	0	0	0	0	1
	RPEO-PLM [38]	0	0	0	0	1
	PSO-EO [36]	0	0	0	0	1
	PSO [36]	0	0	0	0	1
	GA [36]	0.046	0.014	9.93×10^{-4}	0.014	5
	PEO [37]	2.47	2.14	1.85	0.25	6
F_4	APEO	-8.88×10^{-16}	-8.88×10^{-16}	-8.88×10^{-16}	0	1
	RPEO-PLM [38]	-8.88×10^{-16}	-8.88×10^{-16}	-8.88×10^{-16}	0	1
	PSO-EO [36]	-8.88×10^{-16}	-8.88×10^{-16}	-8.88×10^{-16}	0	1
	PSO [36]	-8.88×10^{-16}	-8.88×10^{-16}	-8.88×10^{-16}	0	1
	GA [36]	0.094	0.054	0.03	0.02	5
	PEO [37]	0.12	0.11	0.09	8.4×10^{-3}	6
F_5	APEO	1.21×10^{-19}	4.47×10^{-17}	4.67×10^{-16}	1.15×10^{-16}	1
	RPEO-PLM [38]	3.050×10^{-10}	8.360×10^{-7}	1.050×10^{-5}	2.283×10^{-6}	2
	PSO-EO [36]	9.99×10^{-4}	9.88×10^{-4}	9.54×10^{-4}	2.39×10^{-5}	3
	PSO [36]	26.8	26.0	25.4	0.59	5
	GA [36]	39.7	33.1	30.1	3.95	6
	PEO [37]	9.63	9.42	9.30	0.13	4

4.2. Simulation Study for P-Q Control of Three-Phase Grid-Connected Inverter

In order to demonstrate the effectiveness of the proposed APEO-based P-Q controllers design method, this section presents the simulation results for a 3 kW three-phase grid-connected inverter in a microgrid. The six control parameters of P-Q controllers are tuned by traditional Z-N empirical method [39], AGA [35], PSO [16], and APEO. The system parameters for a three-phase grid-connected inverter are as follows: V_{dc} = 320 V, C_d = 1120 μF, R_f = 0.15 Ω, L_f = 2.5 mH, C_f = 45 μF. The lower and upper limits of the six parameters used in three decoupled PI controllers are set as l_1 = 0.01, l_2 = 30, l_3= 0.01, l_4 = 0.00001, l_5 = 0.00001, l_6 = 0.00001, u_1 = 0.03, u_2 = 50, u_3 = 0.03, u_4 = 10, u_5 = 25, u_6 = 500. The sampling time T_s is set as 2×10^{-6} s and the weights parameters w_1 and w_2 are set as 1 and 1, respectively.

The adjustable parameters of AGA, PSO, and APEO for the optimal design of P-Q controllers used in the following simulations are shown in Table 3. It should be noted that all the simulations have been run on the MATLAB2012b software on a 2.50 GHz PC with an i7-6500U processor running on 8 GB of RAM.

Table 3. The adjustable parameter settings of APEO, PSO, and AGA used for the optimal design of the P-Q controllers in a microgrid.

Algorithm	Parameters Setting
AGA [35]	Population size $N = 30$, $I_{max} = 30$, the crossover probability $p_c = 0.9$, the mutation probability $p_m = 0.1 - 0.01 \times n/N$, where $n = 1, 2,..., N$.
PSO [16]	Population size = 30, $I_{max} = 30$, inertia weight $w = 0.6$, the upper limit of velocity $V_{max} = 0.05$, the lower limit of velocity $V_{min} = -0.05$, acceleration factors $c_1 = 2.0$, $c_2 = 2.0$.
APEO	$N = 30$, $I_{max} = 30$, $b = 0.1$.

4.2.1. Case 1: Under Nominal Condition

In the first case, the reference values of the active and reactive powers for the above described three-phase grid-connected inverter are set as P_{ref} = 2500 W and Q_{ref} = 0 Var. Here, each evolutionary algorithm for the parameters optimization of the P-Q controllers has been implemented for 30 independent runs. Table 4 presents the statistical results of AGA, PSO, and APEO such as the minimum (f_{min}), median (f_{median}), maximum (f_{max}), mean (f_{mean}), and standard deviation (f_{sd}) values of the final global fitness obtained by the30 independent runs. It is clear that the APEO-based P-Q control method is better than the AGA and PSO-based P-Q controllers in terms of all the performance indices.

Table 4. The statistical performance of AGA, PSO, and APEO for designing P-Q controllers.

Algorithm	f_{max}	f_{median}	f_{mean}	f_{min}	f_{sd}
AGA [35]	0.2646	0.2589	0.2586	0.2531	0.0038
PSO [16]	0.2532	0.2495	0.2494	0.2462	0.0023
APEO	0.2434	0.2430	0.2431	0.2427	0.0002

In order to illustrate the convergence characteristics of the proposed method, Figure 4 presents the comparative convergence process of an independent run associated with the f_{min} value shown in Table 4. Clearly, although the best fitness F_{bsest} of APEO is worse than that of AGA and PSO at the beginning because APEO starts its optimization process from a completely random solution, APEO outperforms AGA and PSO after six iterations. The premature convergence of AGA and PSO for the P-Q controller design is very obvious because their best fitness values have not been improved since the third and fourth iteration in AGA and PSO, respectively. Furthermore, Figure 5 presents the evolutionary process of the six P-Q controller parameters in APEO. In conclusion, APEO is better able to explore the problem space of the P-Q controller for a three-phase grid-connected inverter than AGA and PSO.

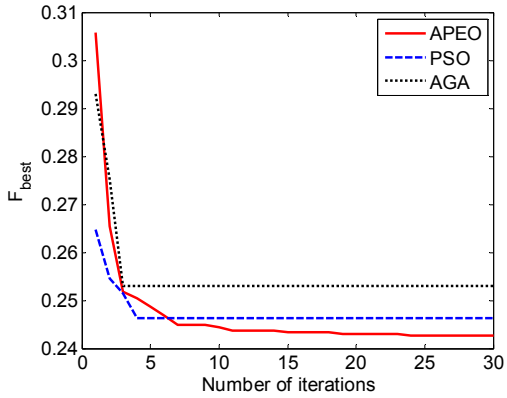

Figure 4. The comparison of the convergence process of APEO, PSO, and AGA for P-Q controllers.

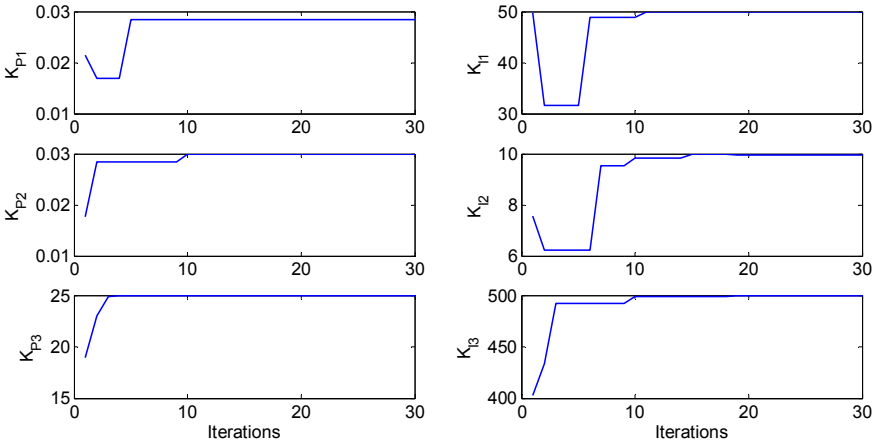

Figure 5. The evolutionary process of the P-Q controller parameters in APEO.

Table 5 presents the best P-Q controller parameters and the corresponding best performance values, including the $f_{\min}$ value, the settling time of the active and reactive powers denoted as t_{sP} and t_{sQ}, respectively, obtained by the traditional Z-N empirical method, AGA, PSO, and APEO. The active and reactive powers under different control parameters obtained by different methods when the DG unit is connected to the grid are compared in Figure 6. It is clear that the t_{sP} and t_{sQ} obtained by APEO are the least among the four methods. In other words, the response of active and reactive powers obtained by APEO is faster than those by the other methods.

Table 5. The parameters of the best-decoupled PI controllers and the corresponding best performance obtained by different P-Q control methods.

Algorithm	K_{po1}	K_{io1}	K_{po2}	K_{io2}	K_{po3}	K_{io3}	$F_{\min}$	T_{sP}(s)	T_{sQ}(s)
Z-N method	0.0219	31.4093	0.0292	2.8040	10.7959	303.2478	0.6870	0.0501	0.0783
AGA	0.0242	41.4078	0.0267	7.1365	24.7489	429.25268	0.2531	0.0406	0.0582
PSO	0.0299	30	0.03	10	25	500	0.2462	0.0450	0.0461
APEO	0.0285	49.9947	0.0299	9.9600	24.9999	499.9615	0.2427	0.0324	0.0375

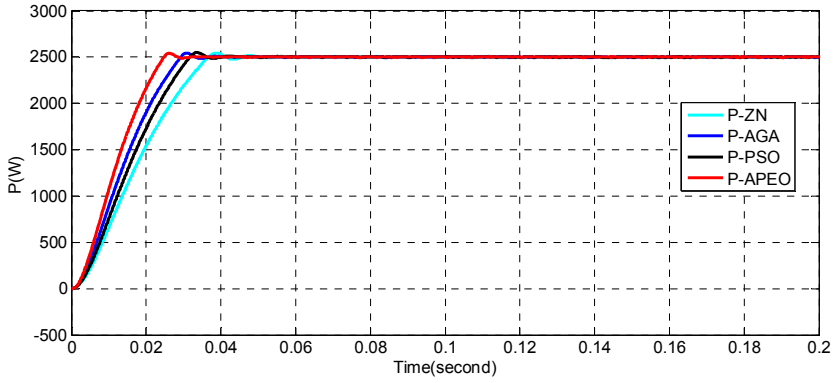

(**a**) Active power

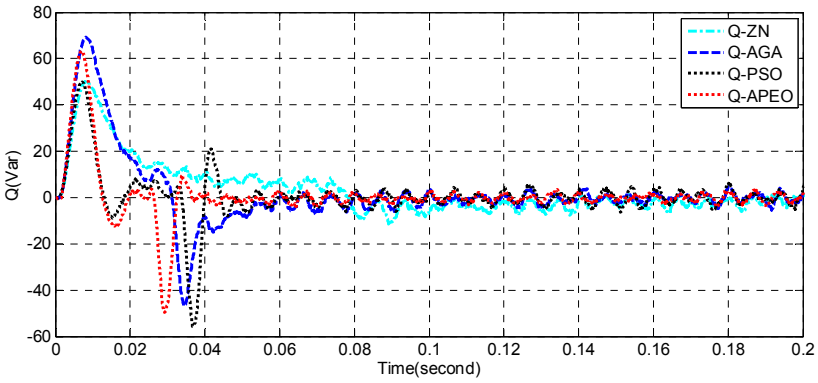

(**b**) Reactive power

Figure 6. The comparison of active (**a**) and reactive (**b**) power obtained by different methods when the distributed generation (DG) unit is connected to the grid.

4.2.2. Case 2: Robustness Test

In order to test the robustness against the variable reference values P_{ref} of different methods, this subsection presents the comparison of the dynamic response of the active and reactive powers under different control parameters obtained by the Z-N empirical method, AGA, PSO, and APEO under the variable reference values of the active power. Here, the variable conditions of the reference active power values are set as the P_{ref} value increases suddenly from 500 W to 2500 W at 0.10 s while P_{ref} decreases suddenly from 2500 W to 500 W at 0.20 s. The dynamic response of the active and reactive powers are compared in Figure 7. The overshoots and settling times of the active and reactive powers obtained by APEO are all the least among the four methods under P_{ref} variance.

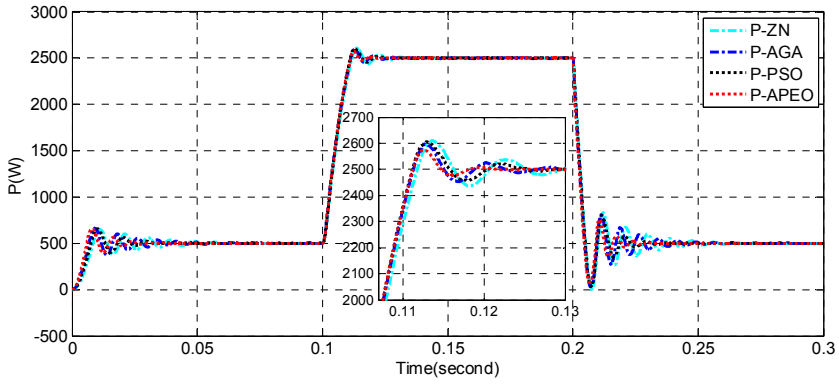

(**a**) Active power

Figure 7. *Cont.*

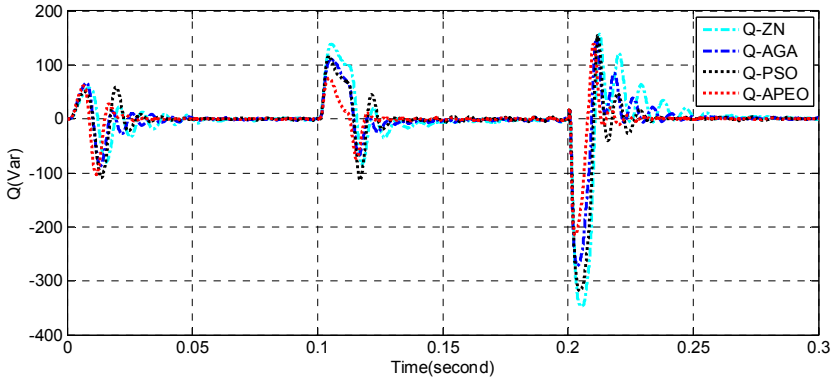

(**b**) Reactive power

Figure 7. The dynamic response of the active (**a**) and reactive (**b**) powers under different control parameters obtained by different methods when the set value of the active power P_{ref} increases suddenly from 0.5 kW to 2.5 kW at 0.10 s and decreases suddenly from 2.5 kW to 0.5 kW at 0.20 s.

5. Experimental Results

IN order to further demonstrate the superiority of the proposed APEO-based P-Q control method compared to the traditional Z-N method, AGA, and PSO-based P-Q controllers design method, this section presents the experimental results on a real 3 kW three-phase grid-connected inverter. The system parameters of the three-phase grid-connected inverter are the same as those in the simulation studies. Figure 8 shows the experimental platform for the P-Q control of a three-phase grid-connected inverter in a microgrid.

Figure 8. The experimental platform of the P-Q control for three-phase grid-connected inverters in a microgrid.

Two experiments have been designed to compare the performance obtained by the traditional Z-N method, AGA, and PSO-based P-Q controllers design methods when the reference value of the active power P_{ref} increases suddenly from 500 W to 2500 W and decreases suddenly from 2500 W to 500 W. The P-Q controller parameters are the same as those shown in Table 3. The experimental dynamic response of the active and reactive powers obtained by the Z-N method, AGA, PSO, and APEO are shown in Figures 9–12, respectively. It is evident that the fluctuation of the experimental active and reactive power obtained by APEO is the least while the fluctuation obtained by Z-N method

is the worst. In other words, the transient performance including the overshoots and settling time of the active and reactive powers obtained by APEO are all the best. On the other hand, the experimental results have also indicated that the P-Q control performance obtained by an evolutionary algorithm such as AGA, PSO, and APEO is obviously better than the traditional Z-N empirical method.

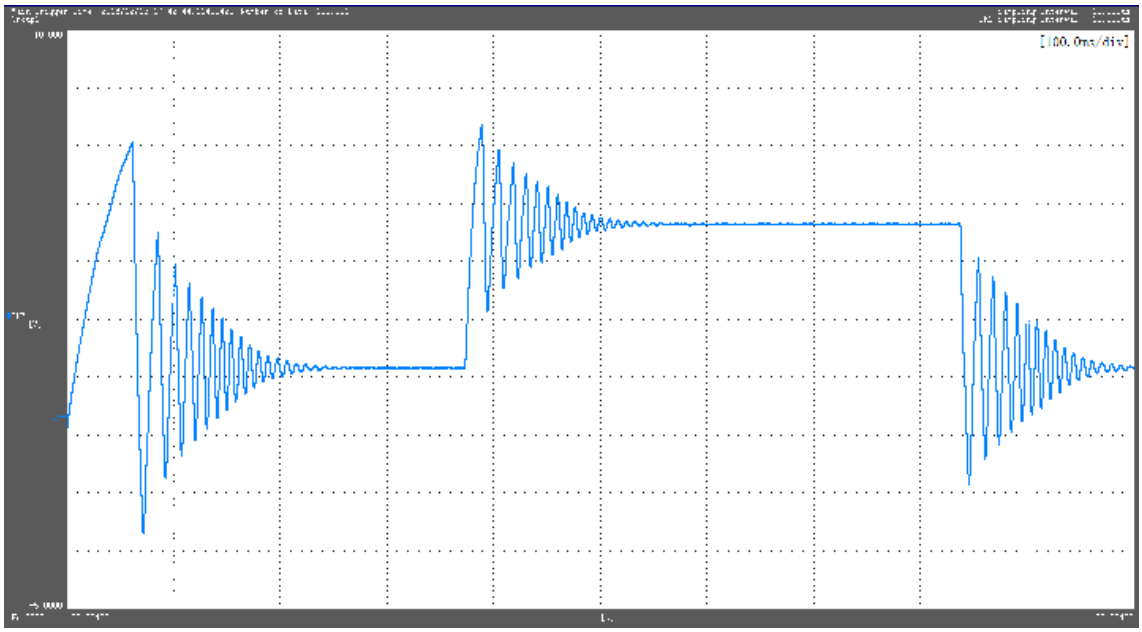

(**a**) The active power P obtained by theZ-N empirical method (P: 0.8kW/div, time: 100ms/div)

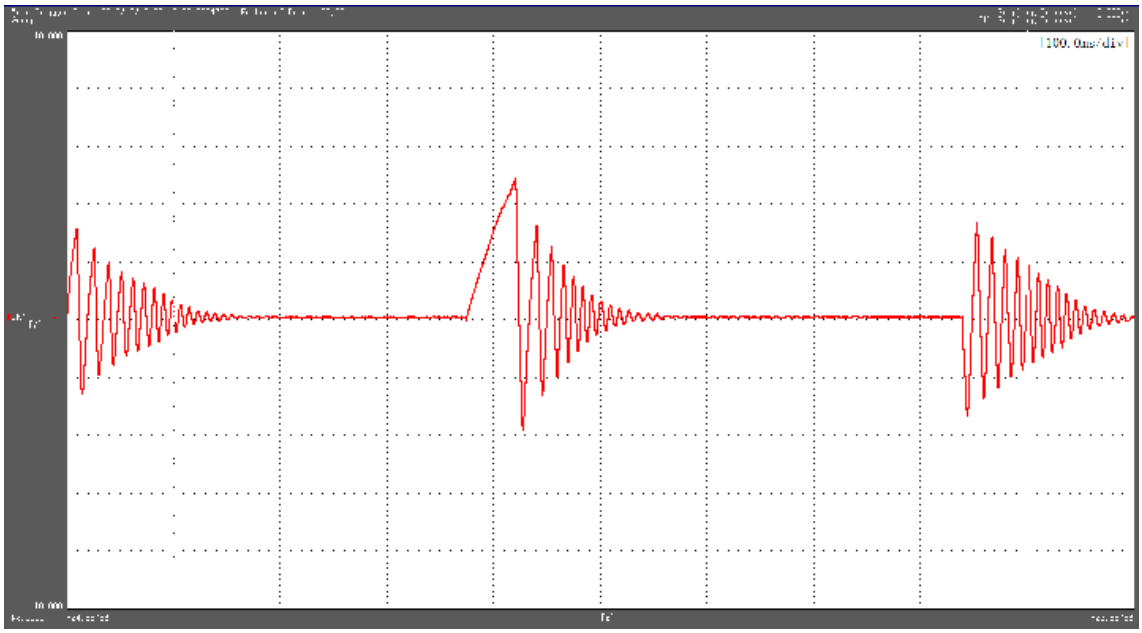

(**b**) The reactive power Q obtained by theZ-N empirical method (Q: 0.3kVar/div, time: 100ms/div)

Figure 9. The experimental dynamic response of the active and reactive powers obtained by the Z-N empirical method when the reference value of the active power P_{ref} increases suddenly from 0.5 kW to 2.5 kW and decreases suddenly from 2.5 kW to 0.5 kW.

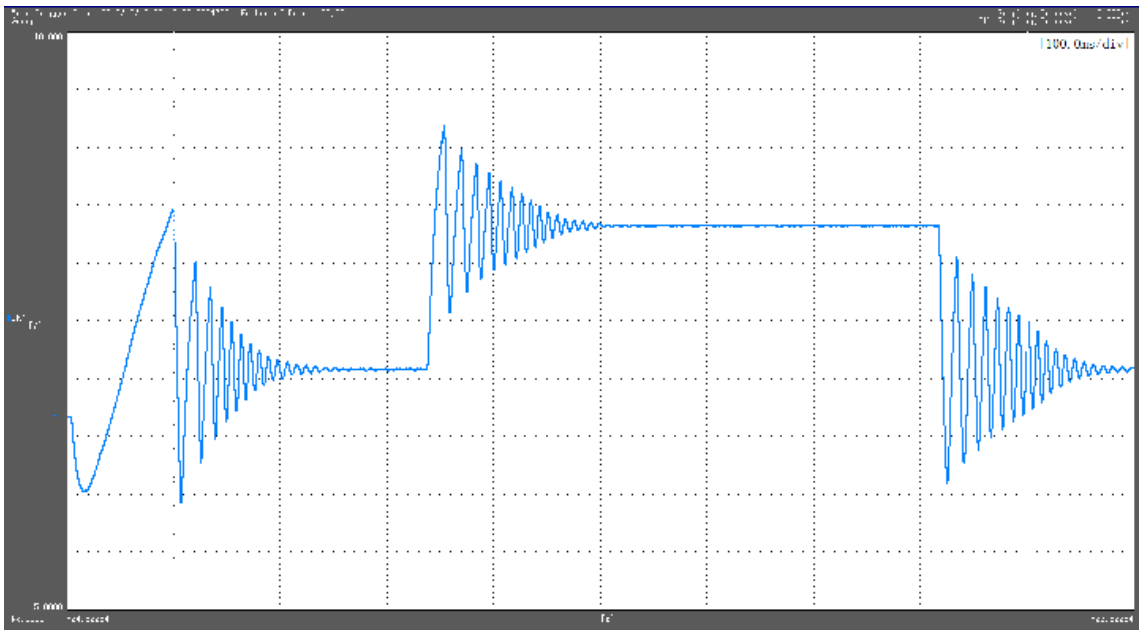

(**a**) The active power P obtained by AGA(P: 0.8kW/div, time: 100ms/div)

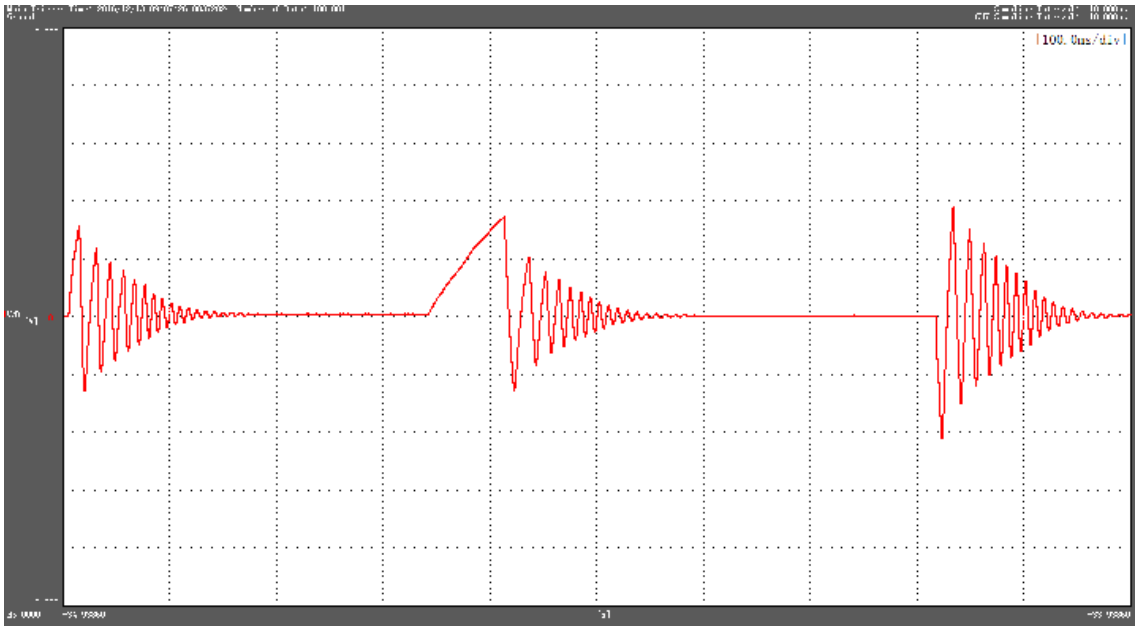

(**b**) The reactive power Q obtained by AGA (Q: 0.3kVar/div, time: 100ms/div)

Figure 10. The experimental dynamic response of the active and reactive powers obtained by AGA when the reference value of the active power P_{ref} increases suddenly from 0.5 kW to 2.5 kW and decreases suddenly from 2.5 kW to 0.5 kW.

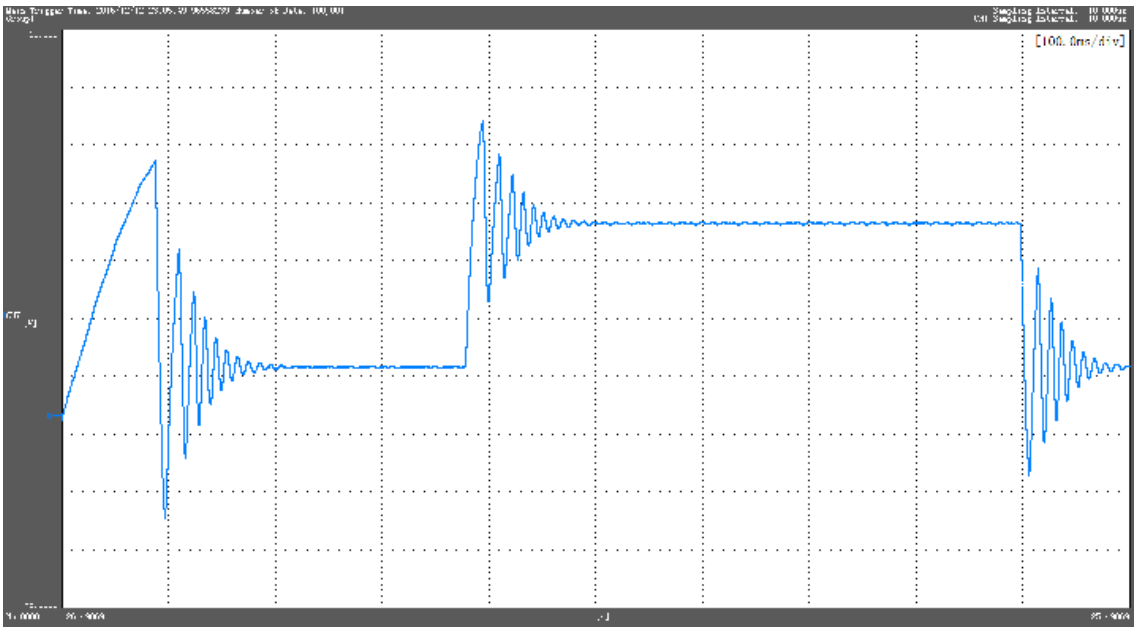

(**a**) The active power P obtained by PSO (P: 0.8kW/div, time: 100ms/div)

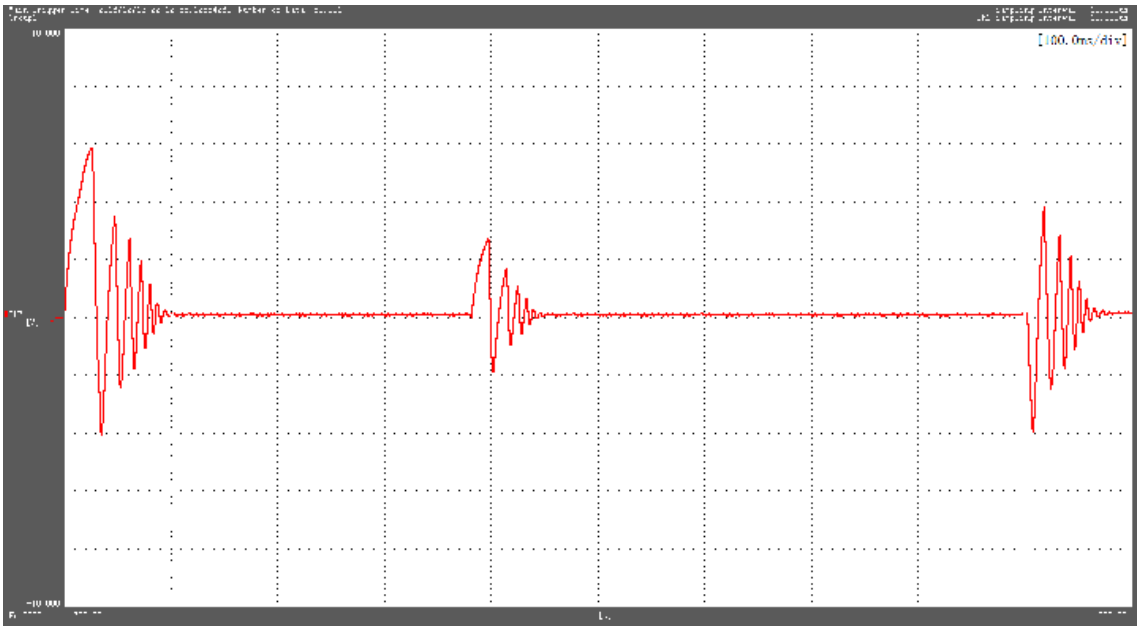

(**b**) The reactive power Q obtained by PSO (Q: 0.3kVar/div, time: 100ms/div)

Figure 11. The experimental dynamic response of the active and reactive powers obtained by PSO when the reference value of the active power P_{ref} increases suddenly from 0.5 kW to 2.5 kW and decreases suddenly from 2.5 kW to 0.5 kW.

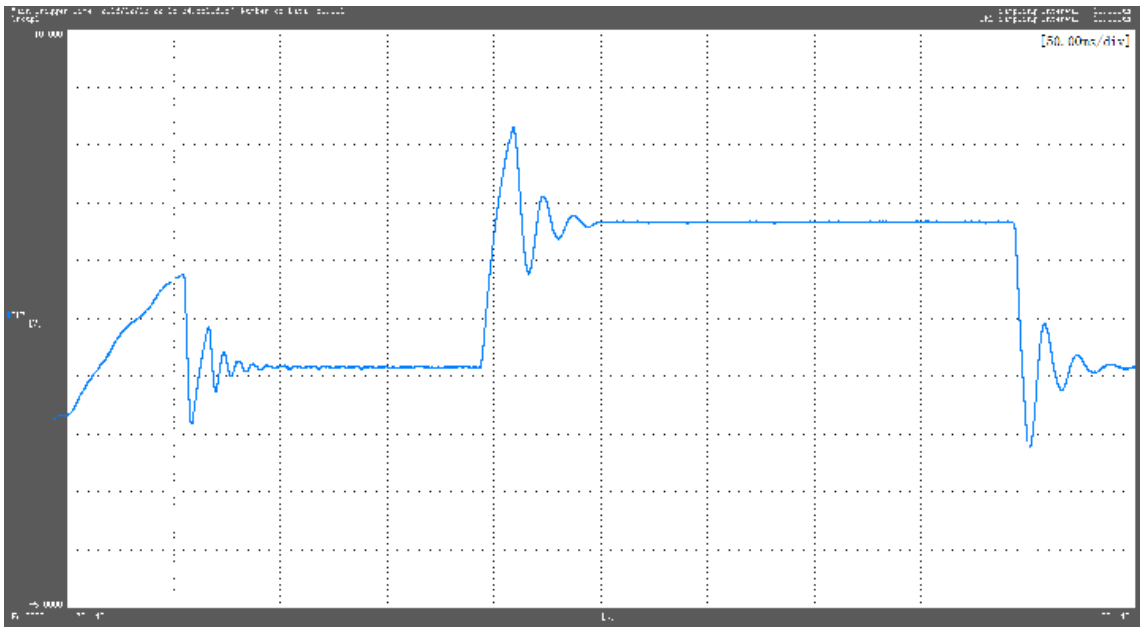

(**a**) The active power P obtained by APEO (P: 0.8kW/div, time: 50ms/div)

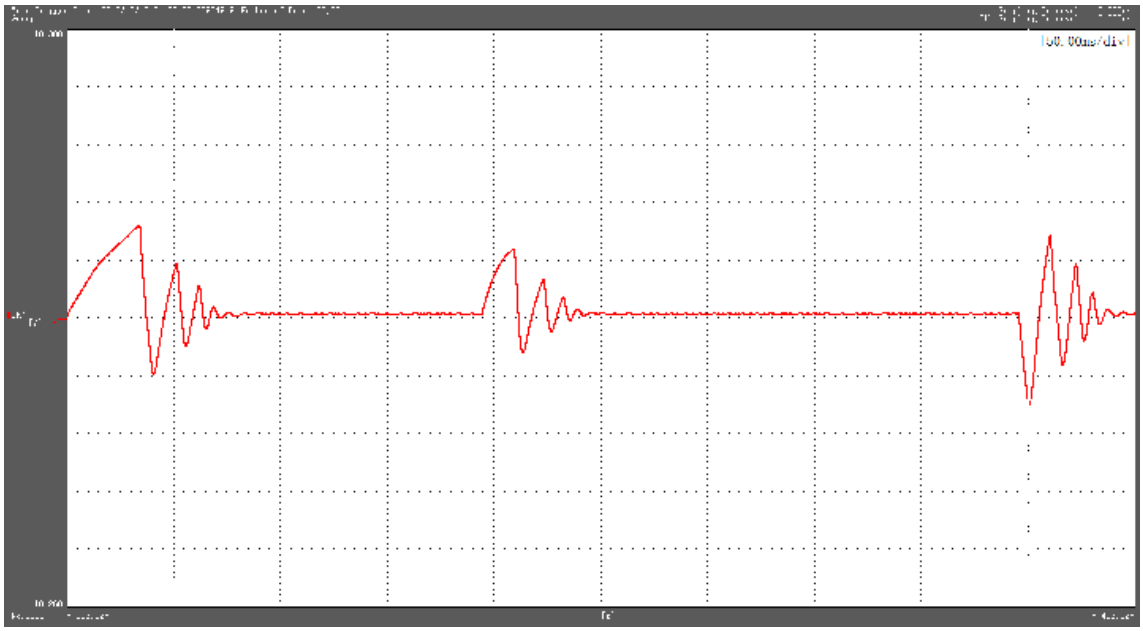

(**b**) The reactive power Q obtainedby APEO (Q: 0.3kVar/div, time: 50ms/div)

Figure 12. The experimental dynamic response of the active and reactive powers obtained by APEO when the reference value of the active power P_{ref} increases suddenly from 0.5 kW to 2.5 kW and decreases suddenly from 2.5 kW to 0.5 kW.

The above experimental results of active and reactive power responses obtained by different methods are slightly worse than the corresponding results, but the superiority of the APEO-based P-Q control method to other methods is still demonstrated by these experimental results. The difference between the simulation and experimental results is due to the ideal characteristics of the three-phase transformer used in the simulations. In fact, the experimental P-Q control performance of a real three-phase grid-connected inverter in a microgrid is further improved by adopting more effective evolutionary algorithms and other advanced control structure, e.g., model predictive control.

6. Conclusions and Open Problems

This paper presents a novel APEO-based intelligent decoupled P-Q control method for the optimal P-Q control issue of three-phase grid-connected inverters in a microgrid. The key ideas behind this proposed APEO-based P-Q control method include encoding six parameters of three decoupled PI controllers in a P-Q controller as the real-coded decision variables, evaluating the control performance of a P-Q controller by considering the integral time absolute error (ITAE) between the output and referenced active power and the ITAE between the output and referenced reactive power, and updating the population by using selection and MNUM operations. The APEO-based P-Q control method is simpler than the existing popular evolutionary algorithms such as AGA-based [35] and PSO-based P-Q control algorithms [16] because of the fewer adjustable parameters and simpler operations in the population-based iterated optimization mechanism of the APEO-based P-Q control method. Furthermore, the simulation and experimental results for a 3 kW three-phase grid-connected inverter in a microgrid have demonstrated that the proposed APEO-based P-Q controller is superior to the traditional Z-N empirical method [39], AGA-based P-Q controllers [35], and PSO-based [16] P-Q controllers in terms of the control performances under nominal and variable control objective conditions. As a consequence, the proposed APEO-based P-Q controller design method can be considered as a promising intelligent P-Q control method for the optimal P-Q control issue of power converters in practical engineering systems. Of course, the P-Q controllers of three-phase grid-connected inverters can be optimized by other theoretical PID methods [40]. However, the P-Q control performance of three-phase grid-connected inverters can be further improved by adopting multi-objective evolutionary algorithms. Additionally, in future, how to extend the basic idea of the APEO-based P-Q controller to more complex power converters and power systems will be studied.

Author Contributions: M.-R.C. presented the problem formulation and designed the main algorithm; H.W. implemented the experiments and analyzed the experimental results; G.-Q.Z. proposed the novel idea behind the proposed method; Y.-X.D. analyzed the simulation results; D.-Q.B. designed the experimental platform. All authors approved the final manuscript.

Funding: This work was partially supported by Zhejiang Provincial Natural Science Foundation of China (Nos. LY16F030011 and LZ16E050002), and National Natural Science Foundation of China (Nos. 51207112 and 61373158).

Acknowledgments: The authors gratefully acknowledge the helpful comments and suggestions of editors and anonymous reviewers.

Conflicts of Interest: The authors declare no conflict of interest.

References

1. Parhizi, S.; Lotfi, H.; Khodaei, A.; Bahramirad, S. State of the art in research on microgrids: A review. *IEEE Access* **2015**, *3*, 890–925. [CrossRef]
2. Arul, P.G.; Ramachandaramurthy, K.V.; Rajkumar, R.K. Control strategies for a hybrid renewable energy system: A review. *Renew. Sustain. Energy Rev.* **2015**, *42*, 597–608. [CrossRef]
3. Fathima, A.H.; Palanisamy, K. Optimization in microgrids with hybrid energy systems-A review. *Renew. Sustain. Energy Rev.* **2015**, *45*, 431–446. [CrossRef]
4. Guerrero, J.M.; Chandorkar, M.; Lee, T.L.; Loh, P.C. Advanced control architectures for intelligent microgrids, part I: Decentralized and hierarchical control. *IEEE Trans. Ind. Electron.* **2013**, *60*, 1254–1262. [CrossRef]
5. Colak, I.; Kabalci, E.; Fulli, G.; Lazarou, S. A survey on the contributions of power electronics to smart grid systems. *Renew. Sustain. Energy Rev.* **2015**, *47*, 562–579. [CrossRef]
6. Hassan, M.A.; Abido, M.A. Optimal design of microgrids in autonomous and grid-connected modes using particle swarm optimization. *IEEE Trans. Power Electron.* **2011**, *26*, 755–769. [CrossRef]
7. Di Fazio, A.R.; Russo, M.; Valeri, S.; De Santis, M. Sensitivity-based model of low voltage distribution systems with distributed energy resources. *Energies* **2016**, *9*, 801. [CrossRef]

8. Casolino, G.M.; Di Fazio, A.R.; Losi, A.; Russo, M.; De Santis, M. A voltage optimization tool for smart distribution grids with distributed energy resources. In Proceedings of the 2017 AEIT International Annual Conference, Cagliari, Italy, 20–22 September 2017.
9. Dai, M.; Marwali, M.N.; Keyhani, A. Power flow control of a single distributed generation unit. *IEEE Trans. Power Electron.* **2008**, *23*, 343–352. [CrossRef]
10. Li, Y.W.; Kao, C.N. An accurate power control strategy for power-electronics-interfaced distributed generation units operating in a low-voltage multibus microgrid. *IEEE Trans. Power Electron.* **2009**, *24*, 2977–2988.
11. Jang, M.; Mihai, C.; Agelidis, V.G. A single-phase grid-connected fuel cell system based on a boost-inverter. *IEEE Trans. Power Electron.* **2013**, *28*, 279–288. [CrossRef]
12. Fazeli, S.M.; Ping, H.W.; Rahim, N.B.A.; Ooi, B.T. Individual-phase decoupled PQ control of three-phase voltage source converter. *IET Gener. Transm. Distrib.* **2013**, *7*, 219–1228. [CrossRef]
13. Adhikari, S.; Li, F.X. Coordinated V-f and P-Q control of solar photovoltaic generators with MPPT and battery storage in microgrids. *IEEE Trans. Smart Grid* **2014**, *5*, 1270–1281. [CrossRef]
14. Adhikari, S.; Li, F.X.; Li, H.J. PQ and PV Control of Photovoltaic Generators in Distribution Systems. *IEEE Trans. Smart* **2015**, *6*, 2929–2941. [CrossRef]
15. Liu, W.; Gu, W.; Xu, Y.; Wang, Y.; Zhang, K. General distributed secondary control for multi-microgrids with both PQ-controlled and droop-controlled distributed generators. *IET Gener. Transm. Distrib.* **2017**, *11*, 707–718. [CrossRef]
16. Al-Saedi, W.; Lachowicz, S.W.; Habibi, D.; Bass, O. Power flow control in grid-connected microgrid operation using particle swarm optimization under variable load conditions. *Int. J. Electr. Power Energy Syst.* **2013**, *49*, 76–85. [CrossRef]
17. Liu, C.H.; Hsu, Y.Y. Design of a self-tuning PI controller for a STATCOM using particle swarm optimization. *IEEE Trans. Ind. Electr.* **2010**, *57*, 702–715.
18. Al-Saedi, W.; Lachowicz, S.W.; Habibi, D.; Bass, O. Voltage and frequency regulation based DG unit in an autonomous microgrid operation using particle swarm optimization. *Int. J. Electr. Power Energy Syst.* **2013**, *53*, 742–751. [CrossRef]
19. Ambia, M.N.; Hasanien, H.M.; Al-Durra, A.; Muyeen, S.M. Harmony search algorithm-based controller parameters optimization for a distributed-generation system. *IEEE Trans. Power Deliv.* **2015**, *30*, 246–255. [CrossRef]
20. Bak, P.; Sneppen, K. Punctuated equilibrium and criticality in a simple model of evolution. *Phys. Rev. Lett.* **1993**, *71*, 4083–4086. [CrossRef] [PubMed]
21. Boettcher, S.; Percus, A. Nature's way of optimizing. *Artif. Intell.* **2000**, *119*, 275–286. [CrossRef]
22. Boettcher, S.; Percus, A. Optimization with extremal dynamics. *Phys. Rev. Lett.* **2001**, *86*, 5211–5214. [CrossRef] [PubMed]
23. Chen, Y.W.; Zhu, Y.J.; Yang, G.K.; Lu, Y.Z. Improved extremal optimization for the asymmetric traveling salesman problem. *Phys. A Stat. Mech. Appl.* **2011**, *390*, 4459–4465. [CrossRef]
24. Liu, J.M.; Chen, Y.W.; Yang, G.K.; Lu, Y.Z. Self-organized combinatorial optimization. *Expert Syst. Appl.* **2011**, *38*, 10532–10540. [CrossRef]
25. Dai, Y.X.; Wang, H.; Zeng, G.Q. Double closed-loop PI control of three-phase inverters by binary-coded extremal optimization. *IEEE Access* **2016**, *4*, 7621–7632. [CrossRef]
26. Lu, Y.Z.; Chen, Y.W.; Chen, M.R.; Chen, P.; Zeng, G.Q. *Extremal Optimization: Fundamentals, Algorithms, and Applications*; CRC Press & Chemical Industry Press: Boca Raton, FL, USA, 2016.
27. Huo, H.B.; Zhu, X.J.; Cao, G.Y. Design for two-degree-of-freedom PID regulator based on improved generalized extremal optimization algorithm. *J. Shanghai Jiaotong Univ. Sci.* **2007**, *E-12*, 148–153.
28. Zeng, G.Q.; Chen, J.; Dai, Y.X.; Li, L.M.; Zheng, C.W.; Chen, M.R. Design of fractional order PID controller for automatic regulator voltage system based on multi-objective extremal optimization. *Neurocomputing* **2015**, *160*, 173–184. [CrossRef]
29. Zeng, G.Q.; Chen, J.; Chen, M.R.; Dai, Y.X.; Li, L.M.; Lu, K.D.; Zheng, C.W. Design of multivariable PID controllers using real-coded population-based extremal optimization. *Neurocomputing* **2015**, *151*, 1343–1353. [CrossRef]
30. Zeng, G.Q.; Lu, K.D.; Dai, Y.X.; Zhang, Z.J.; Chen, M.R.; Zheng, C.W.; Wu, D.; Peng, W.W. Binary-coded extremal optimization for the design of PID controllers. *Neurocomputing* **2014**, *138*, 180–188. [CrossRef]

31. Zeng, G.Q.; Xie, X.Q.; Chen, M.R.; Weng, J. Adaptive population extremal optimization based PID neural network for multivariable nonlinear control systems. *Swarm Evol. Comput.* **2018**, in press. [CrossRef]
32. Zeng, G.Q.; Liu, H.Y.; Wu, D.; Li, L.M.; Wu, L.; Dai, Y.X.; Lu, K.D. A real-coded extremal optimization method with multi-non-uniform mutation for the design of fractional order PID controllers. *Inform. Technol. Control* **2016**, *45*, 358–375. [CrossRef]
33. Wang, H.; Zeng, G.Q.; Dai, Y.X.; Bi, D.Q.; Sun, J.L.; Xie, X.Q. Design of fractional order frequency PID controller for an islanded microgrid: A multi-objective extremal optimization method. *Energies* **2017**, *10*, 1502. [CrossRef]
34. Erickson, R.W.; Maksimovic, D. *Fundamentals of Power Electronics*; Springer Science & Business Media: Berlin, Germany, 2007.
35. Tang, P.H.; Tseng, M.H. Adaptive directed mutation for real-coded genetic algorithms. *Appl. Soft Comput.* **2013**, *13*, 600–614. [CrossRef]
36. Chen, M.R.; Li, X.; Zhang, X.; Lu, Y.Z. A novel particle swarm optimizer hybridized with extremal optimization. *Appl. Soft Comput.* **2010**, *10*, 367–373. [CrossRef]
37. Chen, M.R.; Lu, Y.Z.; Yang, G.K. Population-based extremal optimization with adaptive Lévy mutation for constrained optimization. *Comput. Intell. Secur. Lect. Notes Comput. Sci.* **2007**, *4456*, 144–155.
38. Li, L.M.; Lu, K.D.; Zeng, G.Q.; Wu, L.; Chen, M.R. A novel real-coded population-based extremal optimization algorithm with polynomial mutation: A non-parametric statistical study on continuous optimization problems. *Neurocomputing* **2016**, *174*, 577–587. [CrossRef]
39. Ang, K.H.; Chong, G.; Li, Y. PID control system analysis, design, and technology. *IEEE Trans. Control Syst. Technol.* **2005**, *13*, 559–576.
40. Liang, M.; Zheng, T.Q. Synchronous PI control for three-phase grid-connected photovoltaic inverter. In Proceedings of the 2010 Chinese Control and Decision Conference, Xuzhou, China, 26–28 May 2010.